Letter

Peltier effect of phonons driven by electromagnetic waves

Hiroaki Ishizuka [1] and Masahiro Sato [2]
[1]*Department of Physics, Tokyo Institute of Technology, Meguro, Tokyo 152-8551, Japan*
[2]*Department of Physics, Chiba University, Chiba 263-8522, Japan*

(Received 4 October 2023; accepted 12 June 2024; published 8 July 2024)

Steady current in metals induces a thermal gradient, a phenomenon known as the Peltier effect. The Peltier effect is one of the fundamental phenomena in the thermoelectric properties of materials and is also used in applications such as refrigerators. In this work, we show that an analogous phenomenon occurs by phonons in a noncentrosymmetric insulator, e.g., ferroelectrics, subject to linearly polarized light. Under light illumination, an energy current of phonons occurs through a nonlinear optical effect similar to the bulk photovoltaic effect. We formulate the nonlinear Peltier coefficient of the energy current carried by phonon photocurrent using nonlinear response theory. From the general formula, we show that the phonon photocurrent occurs only in a noncentrosymmetric system with two or more optical phonon bands. We demonstrate the generation of the energy current using a one-dimensional ion chain with three ions in a unit cell, which predicts the generation of an experimentally observable energy current using available THz-infrared light sources.

DOI: 10.1103/PhysRevB.110.L020303

Introduction. In semiconductors, a steady electric current causes a temperature gradient in a material, which is known as the Peltier effect [Fig. 1(a)] [1,2]. The thermoelectric properties of materials are not only important from the viewpoint of transport phenomena but also for applications such as refrigerators. As the thermoelectric effects are related to the energy current carried by the electric carriers, analogous phenomena can occur by a flow of other quasiparticles, such as magnons and phonons. In fact, a spin current analog of the Seebeck effect called the spin Seebeck effect is observed in magnetic insulators [3,4], in which case magnons and spinons carry the spin angular momentum. On the other hand, as accelerating magnons and phonons by the electromagnetic field is difficult, generating magnon and phonon current is often done by introducing a thermal gradient, such as in the thermal Hall effect experiment [5–17]. Therefore, an analog of the Peltier effect, that is, externally controlling the temperature gradient by inducing the flux of quasiparticles, remains challenging.

A possible solution to controlling the flux of magnons and phonons is to utilize nonlinear optical phenomena in noncentrosymmetric materials. The nonlinear response of bulk materials, especially the bulk photovoltaic effect, has received renewed attention from the viewpoint of application and the nontrivial contribution of electronic structures, such as the Berry phase [18–23]. In addition, recent studies on the optical response in magnetic materials found that the spin current of magnons [24–26] and spinons [27] can be induced by a nonlinear response. As these carriers also carry energy, the Peltier effect of charge-neutral particles may also occur by light illumination [Fig. 1(b)]. Among the charge-neutral quasiparticles in materials, phonons are promising in this prospect as the heat transport in materials is often dominated by phonons [2,28,29]. Hence, a nonlinear response of phonons might be a route to realizing novel thermal functionalities.

In this work, we explore the possibility of the Peltier effect of phonons and attempt to understand its basic properties. Using the nonlinear response theory for bosons [26] as a reference, we formulate a general theory for the light-induced energy current. Based on this theory, we argue that a dc phonon current occurs by illuminating a linearly polarized light to noncentrosymmetric insulators. Unlike the bulk photovoltaic and magnon photovoltaic effects, we show that at least two optical modes (more than three phonon modes, including acoustic modes) are necessary for realizing the Peltier effect of phonons. In the last, using a minimal one-dimensional model, we argue that the magnitude of energy current induced by this mechanism is comparable to those observed in the heat conductivity measurement.

Nonlinear Peltier coefficient. The temperature gradient occurs if a flow of energy or heat occurs in a material. The flow is described by energy current density, which is defined by the continuum equation $\partial_t \rho_E(\boldsymbol{x}, t) + \nabla \cdot \boldsymbol{J}_Q(\boldsymbol{x}, t) = 0$. Here, $\rho_E(\boldsymbol{x}, t)$ and $\boldsymbol{J}_Q(\boldsymbol{x}, t)$ are the energy and energy current densities at position $\boldsymbol{x}$ and time t, respectively. Hence, evaluating the Peltier effect reduces to evaluating the average energy current flowing in the material. Phenomenologically, the energy current induced by a nonlinear optical effect reads

$$J_Q^\lambda(\Omega) = \sum_{\mu,\nu} \int \frac{d\omega}{2\pi} \Pi^{(2)}_{\lambda;\mu\nu}(\Omega; \omega, \Omega - \omega) E_\mu(\omega) E_\nu(\Omega - \omega). \quad (1)$$

Here $J_Q^\lambda(\Omega) = \int J_Q^\lambda(t) e^{-i\Omega t} dt$ and $E_\mu(\omega) = \int E_\mu(t) e^{-i\omega t} dt$ are, respectively, the Fourier transforms of the spatially averaged energy-current density $J_Q^\lambda(t)$ with frequency Ω and the μ component of electric field $E_\mu(t)$ of the applied electromagnetic wave with frequency ω. Note that we approximate the electric-field component of light by the spatially uniform oscillating electric field with a frequency ω lower than the electron gap. The averaged current density is defined as $J_Q^\lambda(t) = \frac{1}{V} \int J_Q^\lambda(\boldsymbol{x}, t) dx^d$ with V being the system volume and d being the dimension of the system. Equation (1) defines the

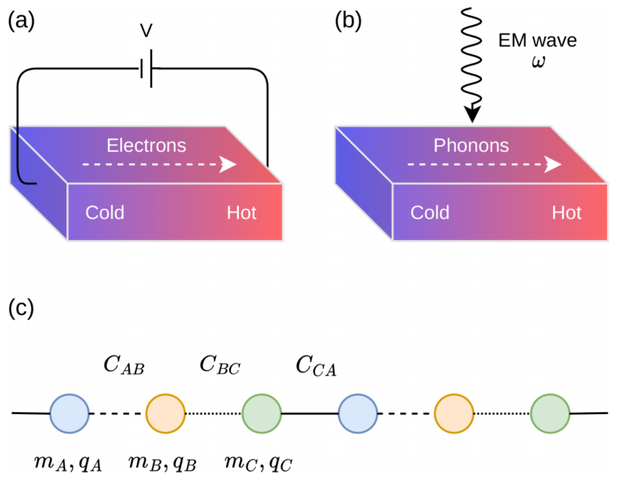

FIG. 1. Schematic of (a) Peltier effect in n-type semiconductor and (b) that by phonon current in insulators. A temperature gradient is induced by electric current in the Peltier effect, whereas phonon current induces the temperature gradient in the Peltier effect of phonons. (c) An example of the noncentrosymmetric insulator in which the Peltier effect of phonon occurs. The blue, orange, and green balls represent A, B, and C sublattice ions, respectively. The m_a and q_a $(a = A, B, C)$ are, respectively, the mass and charge of ath ion, and C_{ab} $(a, b = A, B, C)$ are the strength of quadratic coupling between a and b ions.

nonlinear Peltier coefficient $\Pi^{(2)}_{\lambda;\mu\nu}$, which we study in the rest of this paper.

We note that the nonlinear Peltier effect occurs only in noncentrosymmetric phonon systems. This is shown by the symmetry argument. By acting the inversion operation, the energy current and electric field transforms as $J_Q \to -J_Q$ and $E_\nu \to -E_\nu$. Hence, Eq. (1) transforms $J^\lambda_Q = \Pi^{(2)}_{\lambda;\mu\nu} E_\mu E_\nu \to J^\lambda_Q = -\Pi^{(2)}_{\lambda;\mu\nu} E_\mu E_\nu$. Therefore, similar to the photovoltaic effect in semiconductors, $\Pi^{(2)}_{\lambda;\mu\nu} = 0$ in centrosymmetric systems.

To study the basic properties of energy current carried by phonons, we consider a general low-energy Hamiltonian for phonons of a crystal in d dimension with n_{uc} atoms in a unit cell:

$$\hat{H} = \sum_{ia\mu} \frac{\hat{p}^2_{ia\mu}}{2m_a} + \sum_{ia\mu,jb\nu} \hat{u}_{ia\mu} A_{ia\mu,jb\nu} \hat{u}_{jb\nu}. \tag{2}$$

Here, $A_{ia\mu,jb\nu}$ is the coupling constant, $\hat{u}_{ia\mu}$ is the displacement along the μ axis of $a\,(=1,\cdots,n_{uc})$ sublattice atom in ith unit cell, and $p_{ia\mu}$ is the conjugate momentum of $\hat{u}_{ia\mu}$ satisfying $[\hat{u}_{ia\mu}, \hat{p}_{jb\nu}] = i\hbar\delta_{ij}\delta_{ab}\delta_{\mu\nu}$; $\hbar$ is the Dirac constant. The excitation of $\hat{H}$ is described by free bosons called phonon [30]. Using the phonon representation, $\hat{H}$ reads

$$\hat{H} = \sum_{n,\boldsymbol{k}} \hbar\omega_{n\boldsymbol{k}} \left(\hat{b}^\dagger_{n\boldsymbol{k}} \hat{b}_{n\boldsymbol{k}} + \frac{1}{2} \right), \tag{3}$$

where $\hat{b}_{n\boldsymbol{k}}$ $(\hat{b}^\dagger_{n\boldsymbol{k}})$ is the annihilation (creation) operator of a phonon with band index n and momentum $\boldsymbol{k}$, and $\omega_{n\boldsymbol{k}}$ is the phonon frequency. Here, we define n such that $\omega_{n\boldsymbol{k}} \leqslant \omega_{m\boldsymbol{k}}$ when $n < m$.

We investigate the Peltier effect in this phonon system by calculating the energy current induced by an ac field $E_\mu(t)$. For the sake of generality, we consider an ac perturbation term

$$\hat{H}' = \sum_\mu \hat{B}^\mu E_\mu(t), \tag{4}$$

where the operator $\hat{B}^\mu$ coupled to the field $E_\mu(t)$ is defined as

$$\hat{B}^\mu = \sum_{n,\boldsymbol{k}} \beta^\mu_{n\boldsymbol{k}} \hat{b}_{n\boldsymbol{k}} + \left(\beta^\mu_{n\boldsymbol{k}}\right)^* \hat{b}^\dagger_{n\boldsymbol{k}}, \tag{5}$$

with $\beta^\mu_{n\boldsymbol{k}}$ being the coupling constants. Equation (5) includes most of the basic coupling between the ion charge and the electromagnetic field [31]. For instance, the coupling of ion charge to the spatially uniform electric field $\hat{H}' = -\sum_{i,a,\eta} q_a E_\eta(t) \hat{u}_{ia\eta}$ reads

$$\beta^\mu_{n\boldsymbol{0}} = \sum_a q_a \langle n\boldsymbol{0}\rangle_{a\mu} \sqrt{\frac{\hbar N}{2m_a \omega_{n\boldsymbol{0}}}}, \tag{6}$$

and $\beta^{mu}_{n\boldsymbol{k}\neq\boldsymbol{0}} = 0$. Here, q_a is the charge of ath sublattice ion, m_a is the mass of ath sublattice ion, N is the size of the system, $|n\boldsymbol{k}\rangle$ is the nth eigenmode of dynamical matrix $\tilde{A}_{a\mu,b\nu}(\boldsymbol{k})$, which is an $n_{uc}d \times n_{uc}d$ matrix whose elements are $\tilde{A}_{a\mu,b\nu}(\boldsymbol{k}) = \sum_i \frac{A_{ia\mu,0b\nu}}{\sqrt{m_a m_b}} e^{-i\boldsymbol{k}\cdot(\boldsymbol{r}_{ia}-\boldsymbol{r}_{0b})}$; it corresponds to the eigenvector of nth phonon mode, i.e., $\omega^2_{n\boldsymbol{k}}|n\boldsymbol{k}\rangle = \tilde{A}_{a\mu,b\nu}(\boldsymbol{k})|n\boldsymbol{k}\rangle$.

A general formula for $\boldsymbol{J}_Q$ carried by phonons is given in Ref. [32], in which $\boldsymbol{J}_Q$ is quadratic in the phonon creation and annihilation operators. For the phonon Hamiltonian of Eq. (2), the λ component of the energy current operator reads [32]

$$\begin{aligned} \hat{J}^\lambda_Q = &\sum_{n,m,\boldsymbol{k}} \hat{b}^\dagger_{n\boldsymbol{k}} v^\lambda_{nm}(\boldsymbol{k}) \hat{b}_{m\boldsymbol{k}} + \sum_{n,m,\boldsymbol{k}} \hat{b}^\dagger_{n\boldsymbol{k}} v^\lambda_{n\bar{m}}(\boldsymbol{k}) \hat{b}^\dagger_{m-\boldsymbol{k}} \\ &+ \sum_{n,m,\boldsymbol{k}} \hat{b}_{n-\boldsymbol{k}} v^\lambda_{\bar{n}m}(\boldsymbol{k}) \hat{b}_{m\boldsymbol{k}} + \sum_{n,m,\boldsymbol{k}} \hat{b}_{n-\boldsymbol{k}} v^\lambda_{\bar{n}\bar{m}}(\boldsymbol{k}) \hat{b}^\dagger_{m-\boldsymbol{k}}, \end{aligned} \tag{7}$$

where

$$v^\lambda_{nm}(\boldsymbol{k}) = \frac{\hbar(\omega_{n\boldsymbol{k}} + \omega_{m\boldsymbol{k}})\langle n\boldsymbol{k}|\partial_{k_\lambda}\tilde{A}(\boldsymbol{k})|m\boldsymbol{k}\rangle}{8V\sqrt{\omega_{n\boldsymbol{k}}\omega_{m\boldsymbol{k}}}}, \tag{8}$$

$$v^\lambda_{n\bar{m}}(\boldsymbol{k}) = \frac{\hbar(\omega_{n\boldsymbol{k}} - \omega_{m\boldsymbol{k}})\langle n\boldsymbol{k}|\partial_{k_\lambda}\tilde{A}(\boldsymbol{k})|m\boldsymbol{k}\rangle}{8V\sqrt{\omega_{n\boldsymbol{k}}\omega_{m\boldsymbol{k}}}}, \tag{9}$$

$$v^\lambda_{\bar{n}m}(\boldsymbol{k}) = -\frac{\hbar(\omega_{n\boldsymbol{k}} - \omega_{m\boldsymbol{k}})\langle n\boldsymbol{k}|\partial_{k_\lambda}\tilde{A}(\boldsymbol{k})|m\boldsymbol{k}\rangle}{8V\sqrt{\omega_{n\boldsymbol{k}}\omega_{m\boldsymbol{k}}}}, \tag{10}$$

$$v^\lambda_{\bar{n}\bar{m}}(\boldsymbol{k}) = -\frac{\hbar(\omega_{n\boldsymbol{k}} + \omega_{m\boldsymbol{k}})\langle n\boldsymbol{k}|\partial_{k_\lambda}\tilde{A}(\boldsymbol{k})|m\boldsymbol{k}\rangle}{8V\sqrt{\omega_{n\boldsymbol{k}}\omega_{m\boldsymbol{k}}}}. \tag{11}$$

We note that, in the above equation, we can always take $v^\lambda_{nm}(\boldsymbol{k}) = v^\lambda_{\bar{m}\bar{n}}(-\boldsymbol{k})$, $v^\lambda_{n\bar{m}}(\boldsymbol{k}) = v^\lambda_{m\bar{n}}(-\boldsymbol{k})$, and $v^\lambda_{\bar{n}m}(\boldsymbol{k}) = v^\lambda_{\bar{m}n}(-\boldsymbol{k})$ without reducing the generality. For the sake of convenience, we call $v^\lambda_{nn}(\boldsymbol{k})$ and $v^\lambda_{\bar{n}\bar{n}}(\boldsymbol{k})$ the intraband elements of velocity matrix, and the other terms the interband elements.

The formula for the nonlinear Peltier coefficient is obtained by extending the nonlinear-response theory [26,33] (see also Refs. [34,35] therein). The formula for the dc $(\Omega = 0)$ Peltier coefficient at temperature T reads

$$
\begin{aligned}
&\Pi^{(2)}_{\lambda;\mu\nu}(0;\omega,-\omega)\\
&= -\frac{1}{2\pi\hbar^2}\sum_{\boldsymbol{k},n,m}\frac{\beta^{\mu}_{n\boldsymbol{k}}[v_{n\bar{m}}(\boldsymbol{k})+v_{m\bar{n}}(-\boldsymbol{k})]\beta^{\nu}_{m,-\boldsymbol{k}}}{\left(\omega-\omega_{n\boldsymbol{k}}-\frac{\mathrm{i}}{2\tau}\right)\left(\omega_{n\boldsymbol{k}}+\omega_{m\boldsymbol{k}}+\frac{\mathrm{i}}{2\tau}\right)}\\
&\quad+\frac{1}{2\pi\hbar^2}\sum_{\boldsymbol{k},n,m}\frac{\left(\beta^{\mu}_{n\boldsymbol{k}}\right)^*[v_{\bar{n}m}(-\boldsymbol{k})+v_{\bar{m}n}(\boldsymbol{k})]\left(\beta^{\nu}_{m,-\boldsymbol{k}}\right)^*}{\left(\omega+\omega_{n\boldsymbol{k}}-\frac{\mathrm{i}}{2\tau}\right)\left(\omega_{n\boldsymbol{k}}+\omega_{m\boldsymbol{k}}-\frac{\mathrm{i}}{2\tau}\right)}\\
&\quad+\frac{1}{2\pi\hbar^2}\sum_{\boldsymbol{k},n,m}\frac{\beta^{\mu}_{n\boldsymbol{k}}[v_{nm}(\boldsymbol{k})+v_{\bar{m}\bar{n}}(-\boldsymbol{k})]\left(\beta^{\nu}_{m\boldsymbol{k}}\right)^*}{\left(\omega-\omega_{n\boldsymbol{k}}-\frac{\mathrm{i}}{2\tau}\right)\left(\omega_{n\boldsymbol{k}}-\omega_{m\boldsymbol{k}}+\frac{\mathrm{i}}{2\tau}\right)}\\
&\quad-\frac{1}{2\pi\hbar^2}\sum_{\boldsymbol{k},n,m}\frac{\left(\beta^{\mu}_{n\boldsymbol{k}}\right)^*[v_{mn}(\boldsymbol{k})+v_{\bar{n}\bar{m}}(-\boldsymbol{k})]\beta^{\nu}_{m\boldsymbol{k}}}{\left(\omega+\omega_{n\boldsymbol{k}}-\frac{\mathrm{i}}{2\tau}\right)\left(\omega_{n\boldsymbol{k}}-\omega_{m\boldsymbol{k}}-\frac{\mathrm{i}}{2\tau}\right)}. \qquad (12)
\end{aligned}
$$

Here, $\tau=\tau(T)$ is the phenomenological phonon lifetime at T. The absence of boson distribution function is reasonable considering that an arbitrary number of bosons can occupy the same state, which is in contrast to the fermion case. If $\beta^{\nu}_{m\boldsymbol{k}}=0$ for $\boldsymbol{k}\neq\boldsymbol{0}$, which is the case for the uniform electric field, only $\boldsymbol{k}=\boldsymbol{0}$ terms in Eq. (12) contributes to the Peltier effect. Note that, for the coupling in Eq. (6), $\beta^{\mu}_{n\boldsymbol{0}}$ is proportional to the charge of ions. Therefore, $J^{\lambda}_{Q}=0$ if all ions are charge neutral. The general formula with nonzero $\Omega\neq0$ is also given in the Supplemental Material [33]. For the materials with inversion symmetry, one can show that there exists an eigenstate basis such that the numerator of Eq. (12) is zero [33], which shows the necessity of inversion symmetry breaking.

Three-ion chain. As a demonstration, we consider a one-dimensional lattice model with three ions in a unit cell whose ions move only along the chain direction (Fig. 1), i.e., we assume that there are only longitudinal modes. The Hamiltonian reads

$$
\hat{H}=\sum_{i,a}\frac{\hat{p}^2_{ia}}{2M_a}+\frac{1}{2}\sum_{\langle ia,jb\rangle}C_{ab}(\hat{u}_{ia}-\hat{u}_{jb})^2, \qquad (13)
$$

where $\hat{u}_{ia}$ is the displacement of an atom at $a=A,B,C$ sublattice of ith unit cell from its equilibrium position, $\hat{p}_{ia}$ is the momentum conjugate to $\hat{u}_{ia}$, M_a is the mass of atom at a sublattice, and C_{ab} is the coupling constant between the nearest-neighbor a and b sublattice atoms [Fig. 1(c)]. This model has one acoustic and two optical modes, as shown in Figs. 2(a) and 2(b).

Using this model, we computed the phonon Peltier effect. While there are many different mechanisms that couples the ions to electromagnetic waves, for concreteness [31], we focus on the direct coupling of ion charges to the electric field given in Eq. (5). Figures 2(c) and 2(d) show the ω dependence of $\Pi^{(2)}_{1;11}(0,\omega,-\omega)$. Here, we used the constant relaxation time, which is an approximation widely used in related studies [18,20,21]. The Peltier effect of phonons occurs when the frequency of incident light matches the energy of an optical mode ($\omega=\omega_{2\boldsymbol{0}},\omega_{3\boldsymbol{0}}$ for the cases in Fig. 2), similar to the resonance effect. However, no peak exists at $\omega=0$, which corresponds to the energy of the acoustic mode.

Absence of coupling to the acoustic modes. To understand the absence of a resonance peak at $\omega=0$, we look into the acoustic mode terms, $n=1,\cdots$. In the case of a

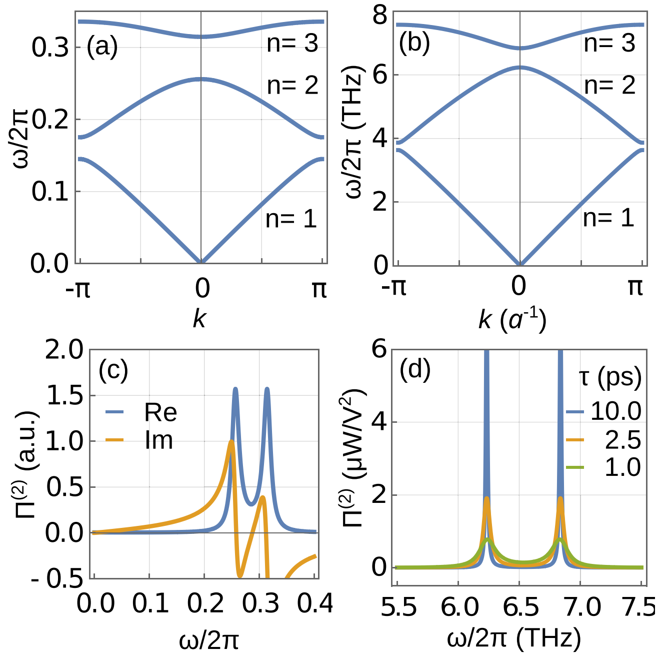

FIG. 2. Phonon bands of the three-ion model with (a) $C_{AB}=C_{BC}=C_{CA}=1$, $M_A=2/3$, $M_B=1$, $M_C=4/3$, and the lattice constant $a_0=1$, and (b) $C_{AB}=C_{CA}=50\,\mathrm{kg/s^2}$, $C_{BC}=40\,\mathrm{kg/s^2}$, $M_A=48$ Da, $M_B=50$ Da, $M_C=52$ Da, and $a_0=4$ Å. (c), (d) The ω dependence of nonlinear Peltier coefficient $\Pi^{(2)}_{x;xx}(0;\omega,-\omega)$. (c) The real and imaginary parts of $\Pi^{(2)}_{x;xx}(0;\omega,-\omega)$ for the model in (a) with the relaxation time $\tau=10$, and (d) the relaxation-time dependence of $\Pi^{(2)}_{x;xx}(0;\omega,-\omega)$ for the model in (d).

translationally symmetric system, $\beta^{\mu}_{n\boldsymbol{0}}$ for acoustic modes become $\beta^{\mu}_{n\boldsymbol{0}}\propto\sum_b q_b$ for the $\hat{H}'$ in Eq. (5) [33]. Hence, in Eq. (12), we can effectively neglect the contribution from acoustic modes in a charge-neutral system, i.e., when $\sum_a q_a=0$. In this case, the summations in Eq. (12) can be replaced by the summation over optical modes only;

$$
\sum_{m,n}\to\sum_{m,n}^{\mathrm{opt}}.
$$

Thereby, the nonlinear Peltier effect occurs only in materials with optical modes.

Interband terms in velocity. We also note that the phonon dispersion in Fig. 2(a) is symmetric about the $k=0$ line, which indicates that the group velocity of excited phonons, $\partial_k\omega_{nk}$, is zero at $k=0$; hence, the diagonal terms in Eq. (7) are zero. The observation implies that the nonlinear Peltier effect occurs not by the selective excitation of phonons with a finite velocity but by some other mechanism. To provide a physical intuition, we point out that Eq. (12) becomes

$$
\begin{aligned}
&\bar{\Pi}^{(2)}_{\nu\mu\mu}(0;\omega,-\omega)\\
&=\frac{1}{2\pi V}\sum_{n}\left[\frac{2\tau}{1+4\tau^2(\omega-\omega_{n\boldsymbol{0}})^2}+\frac{2\tau}{1+4\tau^2(\omega+\omega_{n\boldsymbol{0}})^2}\right]\\
&\quad\times\omega_{n\boldsymbol{0}}\left[\partial_{k_\nu}\phi^{\mu}_{n\boldsymbol{k}}+a^{\nu}_{nn}(\boldsymbol{k})\right]_{\boldsymbol{k}=\boldsymbol{0}}\left|\beta^{\mu}_{n\boldsymbol{0}}\right|^2, \qquad (14)
\end{aligned}
$$

for the coupling in Eq. (6), where $\beta^{\mu}_{n\boldsymbol{k}} = |\beta^{\mu}_{n\boldsymbol{k}}|e^{i\phi^{\nu}_{n\boldsymbol{k}}}$ and $a^{\lambda}_{nn}(\boldsymbol{k}) = \mathrm{i}\langle n\boldsymbol{k}|\partial_{k_\lambda}|n\boldsymbol{k}\rangle$ is the Berry connection of phonons [36,37]. The formula for a more general case is given in the Supplemental Material [33].

This formula resembles that of shift current, in which the photocurrent is related to the intracell position of electron [18,19]. Similarly, $a^{\lambda}_{nn}(\boldsymbol{k})$ is understandable as the center of lattice vibration [33]. Unlike the electron shift current, which is related to the difference of Berry connections of valence and conduction bands, the phonon Peltier effect is related to the Berry connection $a^{\mu}_{nn}(\boldsymbol{k})$ of one photo-excited phonon. The difference between the formulas for the shift current and phonon Peltier effect reflects the difference in physical processes. In view of the many-body wave function, creating a phonon corresponds to enhancing lattice vibration. In noncentrosymmetric materials, the enhanced lattice vibration may occur asymmetrically, which is related to $a^{\mu}_{nn}(\boldsymbol{k})$. Hence, the energy current is related to the intracell position of the excited phonon. The phonon Peltier effect discussed here is another phenomenon related to the nontrivial optical transition, not described by the selective excitation of a phonon with a finite velocity.

We note that a contribution similar to the nonlinear Peltier effect is known in the spin photocurrent [25,27]. However, as the phonon energy current is related to the interband elements, multiple optical modes are necessary for realizing the Peltier effect of phonons (the acoustic modes do not contribute to the Peltier effect as discussed above). In fact, for the Hamiltonian in Eq. (2), one can show that the group velocity at $\boldsymbol{k} = \boldsymbol{0}$, $v^{\lambda}_{nn}(\boldsymbol{0})$ is zero if the phonon bands are nondegenerate at $\boldsymbol{k} = \boldsymbol{0}$; therefore, the intraband contribution vanishes. From a physical viewpoint, the vanishing intraband terms in velocity manifest time-reversal symmetry. Hence, two or more optical bands [at least three bands, including the acoustic mode(s)] are necessary for realizing the Peltier effect of phonons.

Relaxation-time dependence. To gain further insight into the nature of the nonlinear Peltier effect, we next look into the relaxation-time dependence which is relevant to the temperature dependence and magnitude of the Peltier effect. In Eq. (12), the temperature dependence appears in the relaxation time τ. Hence, understanding the temperature dependence of $\Pi^{(2)}$ reduces to analyzing the τ dependence of $\Pi^{(2)}$. Figures 2(b) and 2(d) show the $\Pi^{(2)}$ with different relaxation time τ. The figures show a monotonic increase of $\Pi^{(2)}$ with increasing τ when $\omega = \omega_{n\boldsymbol{0}}$. Indeed, at $\omega = \pm\omega_{n\boldsymbol{0}}$ and $\omega_{n\boldsymbol{k}}\tau \gg 1$, the real part of $\Pi^{(2)}$ in Eq. (12), after assuming only $\boldsymbol{k} = \boldsymbol{0}$ terms contribute, reads

$$\begin{aligned}\mathrm{Re}\big[\Pi^{(2)}_{\lambda;\mu\nu}(0;\pm\omega_{n\boldsymbol{0}},\mp\omega_{n\boldsymbol{0}})\big] &\sim \frac{2\tau}{\pi\hbar^2}\sum_{m(\neq n)}\frac{\mathrm{Im}\big[\beta^{\mu}_{n\boldsymbol{0}}v^{\lambda}_{n\bar{m}}(\boldsymbol{0})\beta^{\nu}_{m\boldsymbol{0}}\big]}{\omega_{n\boldsymbol{0}}+\omega_{m\boldsymbol{0}}}\\ &\quad - \frac{\mathrm{Im}\big[\beta^{\mu}_{n\boldsymbol{0}}v^{\lambda}_{nm}(\boldsymbol{0})\big(\beta^{\nu}_{m\boldsymbol{0}}\big)^{*}\big]}{\omega_{n\boldsymbol{0}}-\omega_{m\boldsymbol{0}}}. \qquad (15)\end{aligned}$$

The τ-linear dependence is distinct from that of the shift current, whose leading order term in τ is independent of τ [18,20]. Rather, it resembles the spin photocurrent using magnetoresonance effect [26], whose spin-current conductivity is proportional to τ. Experimentally investigating the τ dependence via the temperature dependence of τ may provide a route to experimentally delineating the nonlinear Peltier effect from other phenomena.

In the $\tau \to \infty$ limit, the Peltier coefficient reads

$$\begin{aligned}\Pi^{(2)}_{\lambda;\mu\nu}(0;\omega,-\omega) &= \sum_{m\neq n}^{\mathrm{opt}}\frac{\sqrt{\omega_{m\boldsymbol{0}}\omega_{n\boldsymbol{0}}}}{2V\hbar}\beta^{\mu}_{m\boldsymbol{0}}a^{\lambda}_{mn}(\boldsymbol{0})\beta^{\nu}_{n\boldsymbol{0}}\\ &\quad\times\bigg[-\delta(\omega+\omega_{m\boldsymbol{0}})-\delta(\omega-\omega_{m\boldsymbol{0}})\\ &\quad + \mathrm{i}\mathcal{P}\frac{1}{\omega+\omega_{m\boldsymbol{0}}}+\mathrm{i}\mathcal{P}\frac{1}{\omega-\omega_{m\boldsymbol{0}}}\bigg], \qquad (16)\end{aligned}$$

where $a^{\lambda}_{nm}(\boldsymbol{k}) = \mathrm{i}\langle n\boldsymbol{k}|\partial_{k_\lambda}|m\boldsymbol{k}\rangle$ is the non-Abelian Berry connection of phonons, defined in a similar manner to the Abelian Berry connection [36,37]. Here, we used the fact that $a^{\lambda}_{nm}(\boldsymbol{0})$ and $\beta^{\nu}_{n\boldsymbol{0}}$ are real, which holds for Eqs. (2) and (6). The real part of $\Pi^{(2)}_{\lambda;\mu\nu}(0;\omega,-\omega)$ shows a sharp peak at $\omega = \omega_{m\boldsymbol{0}}$, as expected from the relaxation-time dependence.

Magnitude of nonlinear Peltier effect. In the last, we discuss the magnitude of the energy current and the possibility of experimental observation. The results in Fig. 2(d) indicate that the Peltier coefficient is around $\Pi^{(2)} \sim 1\ \ \mu\mathrm{W/V^2}$ at the resonance frequency, which is typically in THz to infrared range. Therefore, assuming the relative electrical permittivity $\epsilon = 10$, the energy-current density induced by an ac electric field of $|E| = 10^5\ \ \mathrm{V/m}$ is $J^{\lambda}_{Q} \sim 10^{-2}\ \ \mathrm{W/cm^2}$. This result should be compared to the energy current measured in thermal conductivity experiments. The energy-current density induced by the temperature gradient can be estimated from the thermal conductivity κ. In the case of an insulator with $\kappa \sim 0.1 - 10$ W/mK, the thermal gradient of $\Delta T = 10^3$ K/m induces $J^{\lambda}_{Q} \sim 10^{-2} - 10^{0}\ \mathrm{W/cm^2}$. As the energy current in our estimate is similar to those measured in thermal transport experiments, the Peltier effect of phonons should induce an observable temperature gradient in candidate materials.

Summary. In this work, we theoretically studied the possibility of the Peltier effect of phonons induced by the illumination of THz to infrared electromagnetic waves. In this phenomenon, the flow of phonons induces energy current, which results in a thermal gradient. However, unlike the Peltier effect by electric current, the phonon current is driven by a nonlinear response similar to the bulk photovoltaic effect. To formulate the Peltier effect, we focused on the energy current of phonons induced by the illumination of electromagnetic waves. The general formula for energy current is derived using the nonlinear response theory. This formula is directly applicable to arbitrary phonon models. Using the formula, we generally showed that at least two optical phonon modes are necessary for inducing the energy current, and the coupling to acoustic mode does not contribute to the phonon Peltier effect. In the last, we demonstrated the Peltier effect using a three-ion model whose phonon bands consist of one acoustic and two optical modes. The result shows that the Peltier effect of phonons occurs when the frequency of the incident electromagnetic wave matches the frequency of optical modes.

The noncentrosymmetric crystal structure, multiple optical modes, and the existence of charged ions are often met in ferroelectrics. Hence, they might be a good candidate for realizing the Peltier effect.

Recently, thermal imaging techniques have enabled spatial resolution of temperature in small devices [38]. As the nonlinear Peltier effect induces a temperature gradient in an isolated device, it should be observable using the thermal imaging method.

Acknowledgments. This work is supported by JSPS KAKENHI (Grants No. JP19K14649, No. JP23K03275, No. JP20H01830, and No. JP20H01849), and by a Grant-in-Aid for Scientific Research on Innovative Areas "Quantum Liquid Crystals" (Grant No. JP19H05825) and "Evolution of Chiral Materials Science using Helical Light Fields" (Grants No. JP22H05131 and No. JP23H04576) from JSPS of Japan.

---

[1] C. Goupil, *Continuum Theory and Modeling of Thermoelectric Elements* (Wiley-VCH, Weinheim, 2016).

[2] A. A. Abrikosov and A. Beknazarov, *Fundamentals of the Theory of Metals* (Dover, New York, 2017).

[3] K. Uchida, H. Adachi, T. Ota, H. Nakayama, S. Maekawa, and E. Saitoh, Observation of longitudinal spin-Seebeck effect in magnetic insulators, Appl. Phys. Lett. **97**, 172505 (2010).

[4] D. Hirobe, M. Sato, T. Kawamata, Y. Shiomi, K. Uchida, R. Iguchi, Y. Koike, S. Maekawa, and E. Saitoh, One-dimensional spinon spin currents, Nat. Phys. **13**, 30 (2017).

[5] C. Strohm, G. L. J. A. Rikken, and P. Wyder, Phenomenological evidence for the phonon Hall effect, Phys. Rev. Lett. **95**, 155901 (2005).

[6] L. Sheng, D. N. Sheng, and C. S. Ting, Theory of the phonon Hall effect in paramagnetic dielectrics, Phys. Rev. Lett. **96**, 155901 (2006).

[7] Y. Kagan and L. A. Maksimov, Anomalous Hall effect for the phonon heat conductivity in paramagnetic dielectrics, Phys. Rev. Lett. **100**, 145902 (2008).

[8] S. Fujimoto, Hall effect of spin waves in frustrated magnets, Phys. Rev. Lett. **103**, 047203 (2009).

[9] H. Katsura, N. Nagaosa, and P. A. Lee, Theory of the thermal Hall effect in quantum magnets, Phys. Rev. Lett. **104**, 066403 (2010).

[10] Y. Onose, T. Ideue, H. Katsura, Y. Shiomi, N. Nagaosa, and Y. Tokura, Observation of the magnon Hall effect, Science **329**, 297 (2010).

[11] R. Matsumoto and S. Murakami, Rotational motion of magnons and the thermal Hall effect, Phys. Rev. B **84**, 184406 (2011).

[12] M. Mori, A. Spencer-Smith, O. P. Sushkov, and S. Maewasa, Origin of the phonon Hall effect in rare-earth garnets, Phys. Rev. Lett. **113**, 265901 (2014).

[13] M. Hirschberger, J. W. Krizan, R. J. Cava, and N. P. Ong, Lager thermal Hall conductivity of neutral spin excitations in a frustrated quantum magnet, Science **348**, 106 (2015).

[14] T. Ideue, T. Kurumaji, S. Ishiwata, and Y. Tokura, Giant thermal Hall effect in multiferroics, Nat. Mater. **16**, 797 (2017).

[15] Y. Kasahara, K. Sugii, T. Ohnishi, M. Shimozawa, M. Yamashita, N. Kurita, H. Tanaka, J. Nasu, Y. Motome, T. Shibauchi, and Y. Matsuda, Unusual thermal Hall effect in a Kitaev spin liquid candidate α-$RuCl_3$, Phys. Rev. Lett. **120**, 217205 (2018).

[16] G. Grissonnanche, A. Legros, S. Badoux, E. Lefrançois, V. Zatko, M. Lizaire, F. Laliberté, A. Gourgout, J.-S. Zhou, S. Pyon, T. Takayama, H. Takagi, S. Ono, N. Doiron-Leyraud, and L. Taillefer, Giant thermal Hall conductivity in the pseudogap phase of cuprate superconductors, Nature (London) **571**, 376 (2019).

[17] T. Saito, K. Misaki, H. Ishizuka, and N. Nagaosa, Berry phase of phonons and thermal Hall effect in nonmagnetic insulators, Phys. Rev. Lett. **123**, 255901 (2019).

[18] R. von Baltz and W. Kraut, Theory of the bulk photovoltaic effect in pure crystals, Phys. Rev. B **23**, 5590 (1981).

[19] B. I. Sturman and V. M. Fridkin, *The Photovoltaic and Photorefractive Effects in Noncentrosymmetric Materials* (Gordon and Breach, Philadelphia, 1992).

[20] J. E. Sipe and A. I. Shkrebtii, Second-order optical response in semiconductors, Phys. Rev. B **61**, 5337 (2000).

[21] S. M. Young, F. Zheng, and A. M. Rappe, First-principles calculation of the bulk photovoltaic effect in bismuth ferrite, Phys. Rev. Lett. **109**, 236601 (2012).

[22] A. M. Cook, B. M. Fregoso, F. de Juan, S. Coh, and J. E. Moore, Design principles for shift current photovoltaics, Nat. Commun. **8**, 14176 (2017).

[23] Y. Tokura and N. Nagaosa, Nonreciprocal responses from noncentrosymmetric quantum materials, Nat. Commun. **9**, 3740 (2018).

[24] I. Proskurin, A. S. Ovchinnikov, J. Kishine, and R. L. Stamps, Excitation of magnon spin photocurrents in antiferromagnetic insulators, Phys. Rev. B **98**, 134422 (2018).

[25] H. Ishizuka and M. Sato, Theory for shift current of bosons: Photogalvanic spin current in ferrimagnetic and antiferromagnetic insulators, Phys. Rev. B **100**, 224411 (2019).

[26] H. Ishizuka and M. Sato, Large photogalvanic spin current by magnetic resonance in bilayer Cr trihalides, Phys. Rev. Lett. **129**, 107201 (2022).

[27] H. Ishizuka and M. Sato, Rectification of spin current in inversion-asymmetric magnets with linearly polarized electromagnetic waves, Phys. Rev. Lett. **122**, 197702 (2019).

[28] A. V. Sologubenko, K. Giannó, H. R. Ott, A. Vietkine, and A. Revcolevschi, Heat transport by lattice and spin excitations in the spin-chain compounds $SrCuO_2$ and Sr_2CuO_3, Phys. Rev. B **64**, 054412 (2001).

[29] T. Kawamata, N. Takahashi, T. Adachi, T. Noji, K. Kudo, N. Kobayashi, and Y. Koike, Evidence for ballistic thermal conduction in the one-dimensional $S = 1/2$ Heisenberg antiferromagnetic spin system Sr_2CuO_3, J. Phys. Soc. Jpn. **77**, 034607 (2008).

[30] G. Grosso and G. P. Parravicini, *Solid State Physics*, 2nd ed. (Academic Press, Cambridge, 2013).

[31] F. Mark, *Optical Properties of Solids* (Clarendon Press, Oxford, 2010).

[32] R. J. Hardy, Energy-flux operator for a lattice, Phys. Rev. **132**, 168 (1963).

[33] See Supplemental Material at http://link.aps.org/supplemental/10.1103/PhysRevB.110.L020303 for the technical details of the presented results.

[34] W. Kraut and R. von Baltz, Anomalous bulk photovoltaic effect in ferroelectrics: A quadratic response theory, Phys. Rev. B **19**, 1548 (1979).

[35] T. Qin, J. Zhou, and J. Shi, Berry curvature and the phonon Hall effect, Phys. Rev. B **86**, 104305 (2012).

[36] L. Zhang, J. Ren, J.-S. Wang, and B. Li, Topological nature of the phonon Hall effect, Phys. Rev. Lett. **105**, 225901 (2010).

[37] T. Qin, Q. Niu, and J. Shi, Energy magnetization and the thermal Hall effect, Phys. Rev. Lett. **107**, 236601 (2011).

[38] K. Uchida, S. Daimon, R. Iguchi, and E. Saitoh, Observation of anisotropic magneto-Peltier effect in nickel, Nature (London) **558**, 95 (2018).